OPTIMAL TWO– AND THREE-DIMENSIONAL EARTH-MOON ORBIT TRANSFERS

E. M. Leonardi[1*], M. Pontani[2]

[1]Faculty of Civil and Industrial Engineering, Sapienza University of Rome, via Eudossiana 18, 00184 Rome, Italy

[2] Department of Astronautical, Electrical, and Energy Engineering, Sapienza University of Rome, via Salaria 851, 00138 Rome, Italy

*e.leonardi@hotmail.it, mauro.pontani@uniroma1.it

ABSTRACT

The determination of minimum-propellant-consumption trajectories represents a crucial issue for the purpose of planning robotic and human missions to the Moon in the near future. This work addresses the problem of identifying minimum-fuel orbit transfers from a specified low Earth orbit (LEO) to a low Moon orbit (LMO), under the assumption of employing high-thrust propulsion. The problem at hand is solved in the dynamical framework of the circular restricted three-body problem. First, the optimal two-dimensional LEO-to-LMO transfer is determined. Second, three-dimensional transfers are considered, in a dynamical model that includes the Cassini's laws of lunar motion. The propellant consumption associated with three-dimensional transfers turns out to be relatively insensitive to the final orbit inclination and exceeds only marginally the value of the globally optimal two-dimensional orbit transfer.

Keywords: Earth-Moon missions, Circular restricted three-body problem, lunar orbit dynamics, spacecraft trajectory optimization.

1 INTRODUCTION

In recent years, lunar missions are attracting an increasing interest, in the clear perspective of planning and completing robotic and human missions in the near future. In this context, identifying minimum-propellant-consumption paths represents a crucial issue. Earth-Moon orbit transfers have been investigated by many researchers in the last decades. Most studies employed the planar circular restricted three-body problem [1] as a reasonably accurate model to investigate orbital motion under the simultaneous gravitational attraction of Earth and Moon. A variety of transfer options have been proposed, also using space manifold dynamics [2] or low-thrust propulsion [3,4].

This work is aimed at identifying minimum-fuel two- and three-dimensional orbit transfers from a specified low Earth orbit (LEO) to a low Moon orbit (LMO), under the assumption of employing high-thrust propulsion. The impulsive thrust approximation is adopted to model short-duration powered arcs. The problem at hand is solved in the dynamical framework of the circular restricted three-body problem, which guarantees more satisfactory accuracy in preliminary mission analysis than the patched conic approximation. First, a formulation of the optimal two-dimensional orbit transfer from LEO to LMO is being presented, aimed at defining and investigating all the feasible paths, with the final intent of finding the globally optimal solution. As a second step, three-dimensional transfers are being considered, in a dynamical framework that includes also the Cassini's laws of lunar motion.

2 THE CIRCULAR RESTRICTED THREE-BODY PROBLEM

In the circular restricted three-body problem (CR3BP), two primary bodies (i.e., Earth and Moon in this study) describe counterclockwise circular orbits around the center of mass of the system, with constant angular speed $\omega = \sqrt{G(m_E + m_M)/R_{EM}^3}$ [1], where G is the universal gravitation constant, R_{EM} is the constant distance between the two primaries, whereas m_E and m_M represent the masses of Earth and Moon, respectively. They attract a third body (the spacecraft) without being attracted by it. This means that the masses m_E, m_M, and m fulfill the inequalities $m_E > m_M >> m \approx 0$. Moreover, canonical units are employed, i.e. the time unit (TU) and the distance unit DU defined as 1 DU = R_{EM} and 1 TU $= \omega^{-1}$. For the Earth-Moon system 1 TU = 375190 s and 1 DU = 384400 km. Moreover, the parameter $\mu := m_M/(m_M + m_E)$ (= 0.012155 for the system at hand) is introduced, and the gravitational parameters of the two primaries can be written as $\mu_E = 1 - \mu$ and $\mu_M = \mu$ (in DU^3/TU^2). Their position along the x-axis is given by $x_E = -\mu$ and $x_M = (1 - \mu)$ (DU).

The synodic reference frame, associated with unit vectors $\left(\hat{\imath}, \hat{\jmath}, \hat{k}\right)$ rotates together with the Earth-Moon system, and the spacecraft is subject to the following dynamics equations:

$$\ddot{x} - 2\omega\dot{y} = \frac{\partial U}{\partial x} \qquad \ddot{y} + 2\omega\dot{x} = \frac{\partial U}{\partial y} \qquad \ddot{z} = \frac{\partial U}{\partial z}, \qquad U := \frac{\omega\left(x^2 + y^2\right)}{2} + \frac{\mu_M}{\sigma} + \frac{\mu_E}{\rho} \tag{1}$$

where (x,y,z) are the position coordinates in the synodic frame, whereas σ and ρ denote the instantaneous spacecraft distance from the center of Moon and Earth, respectively. The inertial frame, aligned with the right-hand sequence of unit vectors $(\hat{c}_1, \hat{c}_2, \hat{c}_3)$, is such that $\hat{c}_3 \equiv \hat{k}$ and $(\hat{c}_1, \hat{c}_2, \hat{c}_3) \equiv \left(\hat{\imath}, \hat{\jmath}, \hat{k}\right)$ at a reference time, set to 0. This circumstance allows expressing the components of the inertial velocity $\boldsymbol{v}$ along $\left(\hat{\imath}, \hat{\jmath}, \hat{k}\right)$ as

$$V_x = \dot{x} - \omega y \qquad V_y = \dot{y} + \omega x \qquad V_z = \dot{z} \tag{2}$$

Moreover, in the CR3BP an integral exists [1], i.e. the Jacobi integral, whose expression is

$$C = 2U - \left(\dot{x}^2 + \dot{y}^2 + \dot{z}^2\right) \tag{3}$$

If the Jacobi integral equals C_1 (= 3.1883 DU^2/TU^2), then the zero velocity curves contain the interior collinear libration point. This means that $C = C_1$ represents a limit for feasibility of the transfer from the Earth to the Moon [1], and the minimum initial speed is $v_{min} = \sqrt{2U\left(x_0, y_0, z_0\right) - C_1}$.

3 OPTIMAL TWO-DIMENSIONAL EARTH-MOON TRANSFERS

This section is devoted to identifying the optimal transfer from a circular LEO to a circular coplanar LMO, with altitudes of 463 km and 100 km, respectively. The LEO-LMO orbit transfer problem is investigated under the following assumptions:

(a) the spacecraft trajectory lies entirely on the Moon orbital plane;
(b) the third body perturbations in LEO and LMO are neglected;
(c) the transfer trajectory includes two impulsive changes of velocity:
- a tangential velocity change $\boldsymbol{\Delta v}_{LEO}$ for translunar orbit injection, and
- a second velocity change $\boldsymbol{\Delta v}_{LMO}$ for insertion into the desired LMO.

The optimization problem consists of minimizing the total velocity variation,

$$J = \Delta v_{LEO} + \Delta v_{LMO} \quad \text{where} \quad \Delta v_{LEO} = \left|\Delta \boldsymbol{v}_{LEO}\right| \quad \text{and} \quad \Delta v_{LMO} = \left|\Delta \boldsymbol{v}_{LMO}\right| \tag{4}$$

3.1 Formulation of the problem

This subsection demonstrates that two parameters are sufficient to identify a two-dimensional LEO-LMO orbit transfer, i.e. (a) magnitude of the first velocity change Δv_{LEO}, and (b) the angle δ that separates $\hat{\imath}$ from the position vector of the spacecraft relative to the Earth center at the initial time. After the first velocity change, the coordinates of the spacecraft position and velocity (relative to the synodic frame) are

$$x_0 = x_E + R_{LEO}\cos\delta \quad \text{and} \quad y_0 = R_{LEO}\sin\delta \tag{5}$$

$$\dot{x}_0^+ = \left(\omega R_{LEO} - v_0\right)\sin\delta \quad \text{and} \quad \dot{y}_0^+ = \left(v_0 - \omega R_{LEO}\right)\cos\delta \quad \left(v_0 = \sqrt{\mu_E / R_{LEO}} + \Delta v_{LEO}\right) \tag{6}$$

These values represent the initial conditions for Eq. (1), written in the form of four first-order differential equations and governing the translunar transfer arc. Intersection with the final LMO occurs at t_f, when the spacecraft has coordinates $\left(x_f, y_f\right)$ and position relative to the Moon denoted with $\boldsymbol{r}_{f,M}$. The angle θ between $\boldsymbol{r}_{f,M}$ and $\hat{\imath}$ is given by

$$\sin\theta = \frac{y_f}{R_{LMO}} \quad \text{and} \quad \cos\theta = \frac{x_f - x_M}{R_{LMO}} \tag{7}$$

The desired velocity components $\left(\dot{x}_f^+, \dot{y}_f^+\right)$ after the second velocity change correspond to the velocity along a circular LMO,

$$\dot{x}_f^+ = \mp\sqrt{\mu_M / R_{LMO}}\sin\theta + \omega y_f \quad \text{and} \quad \dot{y}_f^+ = \pm\sqrt{\mu_M / R_{LMO}}\cos\theta - \omega\left(x_f - x_M\right) \tag{8}$$

where for the symbols $\mp$ e $\pm$ the first and second option correspond respectively to counterclockwise and clockwise lunar orbits. Therefore, if $\left(\dot{x}_f^-, \dot{y}_f^-\right)$ denote the components before the second velocity change, then $\Delta v_{LMO} = \sqrt{\left(\dot{x}_f^+ - \dot{x}_f^-\right)^2 + \left(\dot{y}_f^+ - \dot{y}_f^-\right)^2}$.
In the end, the Earth-Moon transfer is proven to be identified by a pair of parameters, i.e. $\left(\Delta v_{LEO}, \delta\right)$. They are sought in the following intervals:

$$3.025\,\frac{\text{km}}{\text{s}} \le \Delta v_{LEO} \le 3.162\,\frac{\text{km}}{\text{s}} \qquad 0 \le \delta \le 2\,\pi \tag{9}$$

where the lower bound for Δv_{LEO} is obtained using the condition $C = C_1$ (cf. Section 2), while the upper bound corresponds to the escape velocity from the Earth gravitational field.

3.2 Method of solution and numerical results

A preliminary graphical study was performed in order to determine a proper range for the parameters around the globally optimal solution. Figure 1 depicts the contour plot of the objective function in the plane $(\Delta v_{LEO}, \delta)$. First of all, a region of values of Δv_{LEO} and δ that allow the intersection with the desired final orbit can be identified. The values located outside this region yield trajectories that do not intersect the LMO (and the objective function is not defined as a result). Moreover, it is apparent that the region where the objective function assumes higher values (highlighted in yellow) is surrounded by two neighboring regions with lower values (in blue). Each of these two regions corresponds to a different direction of the angular momentum of the LMO, that is, counterclockwise or clockwise orbits, associated respectively with the lower and upper bound. The fact that the optimal paths lie on the boundary of feasible trajectories implies that injection into LMO is performed tangentially, analogously to what occurs for the Hohmann transfer in the restricted two-body problem.

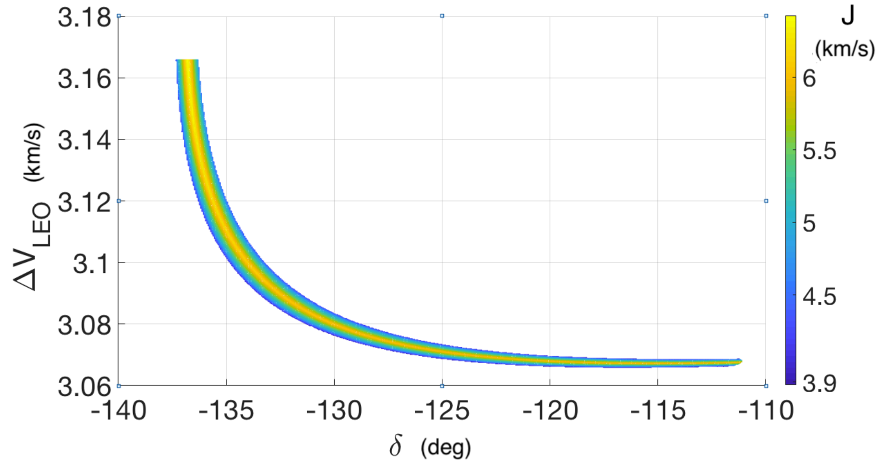

Figure 1: Contour plot of the objective function $\boldsymbol{J(\Delta v_{LEO}, \delta)}$

As a final step, for either clockwise or counterclockwise LMO, the globally optimal solution, corresponding to the minimum propellant consumption, is determined, using the particle swarm algorithm [5]. The solution is located around the lowest values of Δv_{LEO} and the highest values of δ. It is worth remarking that in this region extremely close values of the objective function correspond to relatively different values of δ. This reduced sensitivity of the objective function has practical implications, because relatively different directions can be chosen at departure, with modest effects on the overall propellant consumption.
Table 1 collects the results of the optimization process. These are extremely close to those found by Miele and Mancuso [6] in terms of Δv_{LEO}, although they differ with respect to the departure angle δ. However, these results are slightly more accurate than those in Ref. 6, where the authors identified the center of the Earth with the center of the entire system. Figure 2 portrays the transfer trajectory for both counterclockwise and clockwise arrival at LMO.

	J (km/s)	Δv_{LEO} (km/s)	δ (deg)
Clockwise	3.885	3.069	-117.52
Counterclockwise	3.878	3.066	-117.38

Table 1: Globally optimal two-dimensional LEO-LMO orbit transfers

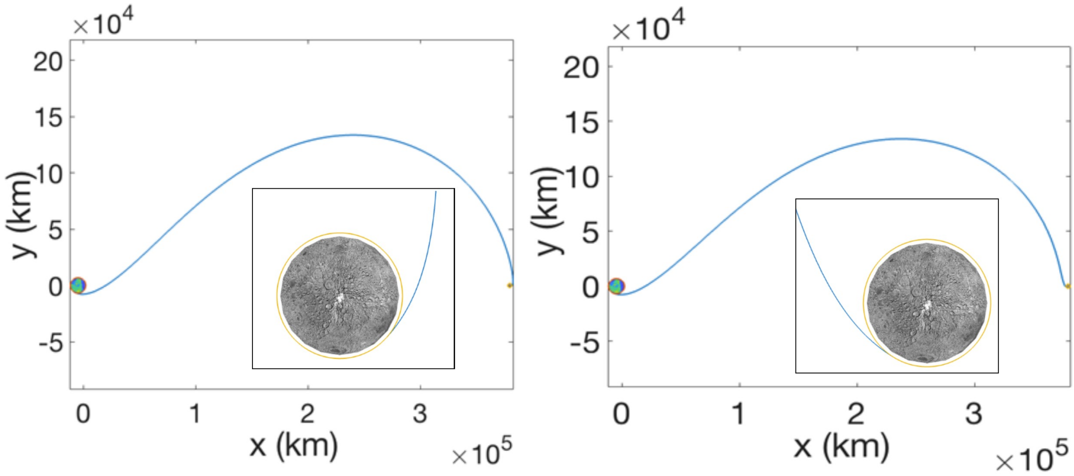

Figure 2: Plot of the 2D-trajectory in $\left(\hat{\imath},\hat{\jmath},\hat{k}\right)$ (a) Clockwise LMO, (b) Counterclockwise LMO

4 OPTIMAL THREE-DIMENSIONAL EARTH-MOON TRANSFERS

This section addresses the determination of the optimal three-dimensional orbit transfer from an initial LEO to a final LMO, both with specified altitude and inclination. Specifically, the initial orbit has altitude of 463 km and inclination of 51.6 deg, whereas different final circular lunar orbits are considered, with common altitude of 100 km and distinct inclinations. Assumptions (b) and (c) of Section 3 still hold, and the optimization problem consists again of minimizing the cost function defined in Eq. (4).

4.1 Reference frames

As a first step, the Earth-centered inertial frame (ECI) and the Moon-centered inertial frame (MCI) are defined in relation to the heliocentric inertial frame (HCI). The latter reference system is associated with the unit vectors $(\hat{c}_1,\hat{c}_2,\hat{c}_3)$, where $\hat{c}_1$ is the vernal axis (corresponding to the intersection of the ecliptic plane with the Earth equatorial plane) and $\hat{c}_3$ points toward the Earth orbit angular momentum [7]. The ECI-frame is associated with the unit vectors $\left(\hat{c}_1^{(E)},\hat{c}_2^{(E)},\hat{c}_3^{(E)}\right)$, where $\hat{c}_1^{(E)}$ is the vernal axis and $\hat{c}_3^{(E)}$ points toward the Earth rotation axis [7]. The ECI-frame and the HCI-frame are related through the ecliptic obliquity angle δ_E $(=23.45\text{ deg})$,

$$\left[\hat{c}_1^{(E)} \quad \hat{c}_2^{(E)} \quad \hat{c}_3^{(E)}\right]^T = \mathbf{R}_1(-\delta_E)[\hat{c}_1 \quad \hat{c}_2 \quad \hat{c}_2]^T \tag{8}$$

where the notation $\mathbf{R}_j(\chi)$ refers to an elementary counterclockwise rotation by angle χ about axis *j*. According to Cassini's laws, the Moon's rotation axis $\hat{z}_M$ is coplanar with the Moon's orbit angular momentum $\boldsymbol{h}_M$ and the normal to the ecliptic plane $\hat{c}_3$. The two vectors $\hat{z}_M$ and $\boldsymbol{h}_M$ are located at opposite sides of the ecliptic pole $\hat{c}_3$, and both of them are subject to clockwise precession due to the Sun, with a period of 18.6 years. Hence, axis $\hat{c}_3^{(M)}$ of the MCI-frame can be properly identified as the rotation axis $\hat{z}_M$ at a reference epoch t_{ref},

$\hat{c}_3^{(M)} = \hat{z}_M\left(t_{ref}\right)$. If ψ_M and δ_M denote respectively the precession angle and the Moon equator obliquity (separating $\hat{c}_3^{(M)}$ from $\hat{c}_3$), then

$$\left[\hat{c}_1^{(M)} \quad \hat{c}_2^{(M)} \quad \hat{c}_3^{(M)}\right]^T = \mathbf{R}_1\left(\delta_M\right)\mathbf{R}_3\left(\psi_M^{(ref)}\right)\left[\hat{c}_1 \quad \hat{c}_2 \quad \hat{c}_2\right]^T \tag{9}$$

where $\psi_M^{(ref)}$ $\left(=-81.7\text{ deg}\right)$ represents the precession angle at t_{ref} (set to 1 June 2029) and $\delta_M = 1.5\text{ deg}$. Because the LEO-LMO transfer completes in a few days, ψ_M is assumed constant and equal to $\psi_M^{(ref)}$. Moreover, the inertial orbital frame $\left(\hat{N}_M, \hat{M}_M, \hat{h}_M\right)$ can be introduced, with unit vectors $\hat{N}_M$ and $\hat{h}_M$ aligned with the ascending node and the angular momentum of the lunar orbit at t_{ref}. This frame is related to $\left(\hat{c}_1^{(E)}, \hat{c}_2^{(E)}, \hat{c}_3^{(E)}\right)$ through the inclination and the RAAN of the lunar orbit at t_{ref},

$$\left[\hat{N}_M \quad \hat{M}_M \quad \hat{h}_M\right]^T = \mathbf{R}_1\left(i_M\right)\mathbf{R}_3\left(\Omega_M\right)\left[\hat{c}_1^{(E)} \quad \hat{c}_2^{(E)} \quad \hat{c}_3^{(E)}\right]^T \tag{10}$$

Finally, the synodic frame aligned with $\left(\hat{\imath}, \hat{\jmath}, \hat{k}\right)$ is related to $\left(\hat{N}_M, \hat{M}_M, \hat{h}_M\right)$ through a single counterclockwise rotation about axis 3 by angle $\alpha := \omega\left(t - \bar{t}\right)$, which means that these two frames are aligned when $t = \bar{t} + 2k\pi/\omega$ $\left(k \in \mathbb{Z}\right)$,

$$\left[\hat{\imath} \quad \hat{\jmath} \quad \hat{k}\right]^T = \mathbf{R}_3\left(\alpha\right)\left[\hat{N}_M \quad \hat{M}_M \quad \hat{h}_M\right]^T \tag{11}$$

The previous definitions remove all the assumptions related to two-dimensional motion that were introduced in Section 3.

4.2 Formulation of the problem

In this study, the three-dimensional LEO-LMO transfer is formulated in terms of three unknown parameters: (a) magnitude of the first velocity change Δv_{LEO}, (b) right ascension of LEO Ω_{LEO}, and (c) the initial phase angle α_i between the synodic reference frame $\left(\hat{\imath}, \hat{\jmath}, \hat{k}\right)$ and the inertial frame $\left(\hat{N}_M, \hat{M}_M, \hat{h}_M\right)$. If t_i denotes the initial time, then $\alpha_i \equiv \omega\left(t_i - \bar{t}\right)$. The initial orbit inclination is instead specified and denoted with i_{LEO}. The unit vector $\hat{h}$, associated with the spacecraft angular momentum prior to departure, can be written in terms of $\left(\Omega_{LEO}, i_{LEO}\right)$,

$$\hat{h} = \left[\sin\Omega_{LEO}\sin i_{LEO} \quad -\cos\Omega_{LEO}\sin i_{LEO} \quad \cos i_{LEO}\right]\left[\hat{c}_1^{(E)} \quad \hat{c}_2^{(E)} \quad \hat{c}_3^{(E)}\right]^T \tag{12}$$

The first tangential impulse is applied at one of the two intersection points between the Moon orbit plane and the LEO, with the intent of injecting the spacecraft into LMO at the opposite intersection point. The line that contains these two points is aligned with the unit vector

$$\hat{r}_0 = \frac{\hat{h}_M \times \hat{h}}{\left|\hat{h}_M \times \hat{h}\right|} \tag{13}$$

Moreover, at departure from the Earth orbit, the local vertical local horizontal frame (LVLH) is associated with the right-hand sequence $\left(\hat{r}_0, \hat{\theta}_0, \hat{h}\right)$, where

$$\hat{\theta}_0 = \hat{h} \times \hat{r}_0 \tag{14}$$

The initial values for the numerical integration of Eq. (1) can be obtained under the assumption that the initial velocity change is applied tangentially, i.e. along $\hat{\theta}_0$. As a result, if $\boldsymbol{v}_E$ denotes the inertial velocity of the Earth in the CR3BP, then the spacecraft inertial velocity in the CR3BP right after the first velocity change is

$$\boldsymbol{v} = v_0 \hat{\theta}_0 + \boldsymbol{v}_E \quad \text{where} \quad v_0 = \sqrt{\mu_E / R_{LEO}} + \Delta v_{LEO} \quad \text{and} \quad \boldsymbol{v}_E = \omega x_E \hat{j} \tag{15}$$

In order to provide the initial conditions for the numerical integration of Eq. (1), the previous relation must be written in the synodic frame. To do this, $\hat{\theta}_0$ is first obtained in the ECI-frame using Eqs. (10) and (12)-(14). Then, Eqs. (10) and (11) are employed to project $\hat{\theta}_0$ in the synodic frame. Once the three components $\left(V_x, V_y, V_z\right)$ of $\boldsymbol{v}$ along $\left(\hat{\imath}, \hat{\jmath}, \hat{k}\right)$ have been identified, the initial conditions $\left(\dot{x}_0^+, \dot{y}_0^+, \dot{z}_0^+\right)$ can be found using Eq. (2). Moreover, the spacecraft position vector at departure, taken from the origin of the Earth- Moon system and denoted with $\boldsymbol{r}_i$, is given by

$$\boldsymbol{r}_i = x_E \hat{\imath} + R_{LEO} \hat{r}_0 \tag{16}$$

Using steps similar to those for $\hat{\theta}_0$, also $\hat{r}_0$ can be projected into the synodic frame $\left(\hat{\imath}, \hat{\jmath}, \hat{k}\right)$, and this leads to identifying the initial conditions for the position coordinates $\left(x_0, y_0, z_0\right)$.

The final conditions at injection correspond to intersection of the transfer arc with the sphere centered at the Moon and with radius equal to that of the final orbit. The related components in the synodic frame are denoted with $\left(x_f, y_f, z_f, \dot{x}_f^-, \dot{y}_f^-, \dot{z}_f^-\right)$. Using Eqs. (9)-(11), the position vector relative to the Moon center, $\boldsymbol{r}_{f,M}$, can be expressed in the MCI-frame as

$$\begin{aligned} \boldsymbol{r}_{f,M} &= \begin{bmatrix} x_f - x_M & y_f & z_f \end{bmatrix}^T \begin{bmatrix} \hat{\imath} & \hat{\jmath} & \hat{k} \end{bmatrix}^T \\ &= \begin{bmatrix} x_f - x_M & y_f & z_f \end{bmatrix}^T \mathbf{A}\left(\alpha_f, i_M, \Omega_M, \delta_E, \psi_M, \delta_M\right) \begin{bmatrix} \hat{c}_1^{(M)} & \hat{c}_2^{(M)} & \hat{c}_3^{(M)} \end{bmatrix}^T \end{aligned} \tag{17}$$

where

$$\mathbf{A}\left(\alpha_f, i_M, \Omega_M, \delta_E, \psi_M, \delta_M\right) := \mathbf{R}_3\left(\alpha_f\right) \mathbf{R}_1\left(i_M\right) \mathbf{R}_3\left(\Omega_M\right) \mathbf{R}_1\left(-\delta_E\right) \mathbf{R}_3^T\left(\psi_M^{(ref)}\right) \mathbf{R}_1^T\left(\delta_M\right) \tag{18}$$

Matrix **A** is the result of several subsequent elementary rotations, $\alpha_f = \alpha_i + \omega \Delta t$, and Δt represents the flight time. The desired orbit plane has specified inclination i_f, whereas its RAAN Ω_f is found by solving the equation $\boldsymbol{r}_{f,M} \cdot \boldsymbol{h}_{f,M} = 0$, after writing $\boldsymbol{h}_{f,M}$ in terms of i_f and Ω_f,

$$\boldsymbol{h}_{f,M} = \left[\sin\Omega_f \sin i_f \quad -\cos\Omega_f \sin i_f \quad \cos i_f\right]\left[\hat{c}_1^{(M)} \quad \hat{c}_2^{(M)} \quad \hat{c}_3^{(M)}\right]^T \tag{19}$$

Using Eqs. (17) and (19), the orthogonality condition $\boldsymbol{r}_{f,M} \cdot \boldsymbol{h}_{f,M} = 0$ assumes the following form :

$$a_1 \cos\Omega_f + a_2 \sin\Omega_f + a_3 = 0 \tag{20}$$

where the terms a_k $(k = 1,2,3)$ depend on $\{x_f, y_f, z_f, \alpha_f, i_M, \Omega_M, \delta_E, \psi_M, \delta_M, i_f\}$. In general, Eq. (20) yields two solutions, and the one associated with the lower value of the objective function is selected. Once the final orbit has been determined, the velocity components $\left(\dot{x}_f^+, \dot{y}_f^+, \dot{z}_f^+\right)$ can be found using steps analogous to those described at the beginning of this section, with $\left(\hat{c}_1^{(M)}, \hat{c}_2^{(M)}, \hat{c}_3^{(M)}\right)$ in place of $\left(\hat{c}_1^{(E)}, \hat{c}_2^{(E)}, \hat{c}_3^{(E)}\right)$. Therefore, if $\left(\dot{x}_f^-, \dot{y}_f^-, \dot{z}_f^-\right)$ denote the components before the second velocity change, then

$$\Delta v_{LMO} = \sqrt{\left(\dot{x}_f^+ - \dot{x}_f^-\right)^2 + \left(\dot{y}_f^+ - \dot{y}_f^-\right)^2 + \left(\dot{z}_f^+ - \dot{z}_f^-\right)^2} \tag{20}$$

In the end, the Earth-Moon transfer is proven to be identified by three parameters, i.e. $\left(\Delta v_{LEO}, \Omega_{LEO}, \alpha_i\right)$. They are sought in the following intervals:

$$3.025 \ \text{km/s} \le \Delta v_{LEO} \le 3.162 \ \text{km/s} \qquad 0 \le \Omega_{LEO} \le 2\pi \qquad 0 \le \alpha_i \le \pi \tag{12}$$

where the lower bound for Δv_{LEO} is obtained again using the condition $C = C_1$ (cf. Section 2), while the upper bound corresponds to the escape velocity from the Earth gravitational field.

4.3 Numerical results

For the problem at hand, the particle swarm algorithm is used, with three unknown parameters $(\Delta v_{LEO}, \alpha_i, \Omega_{LEO})$. The optimization is repeated with different values for the inclination of the LMO, ranging from 10 to 90 deg.

From inspecting the results in Table 2, it is evident that the overall velocity change is only marginally greater than the value found for the two-dimensional transfer. Unsurprisingly, the total velocity change decreases with the inclination of the final lunar orbit. In fact, reaching lunar orbits with lower inclinations requires intercepting the Moon at lower latitudes, resulting in a reduced Δv_{LEO} at translunar injection. It is worth remarking that the selection of the initial optimal RAAN can take advantage of the orbit precession motion due to the Earth oblateness. Moreover, if a final polar LMO with a specific RAAN is desired, this can be achieved in three steps, i.e. (a) selecting a final orbit with lower inclination (e.g., 80 deg), (b) waiting until precession (due to Moon oblateness) changes the RAAN to the desired value, and (c) performing a final out-of-plane maneuver to change the inclination to 90 deg. Figures 3 and 4 portray two optimal LEO-LMO transfers, associated respectively with final lunar polar and equatorial orbits.

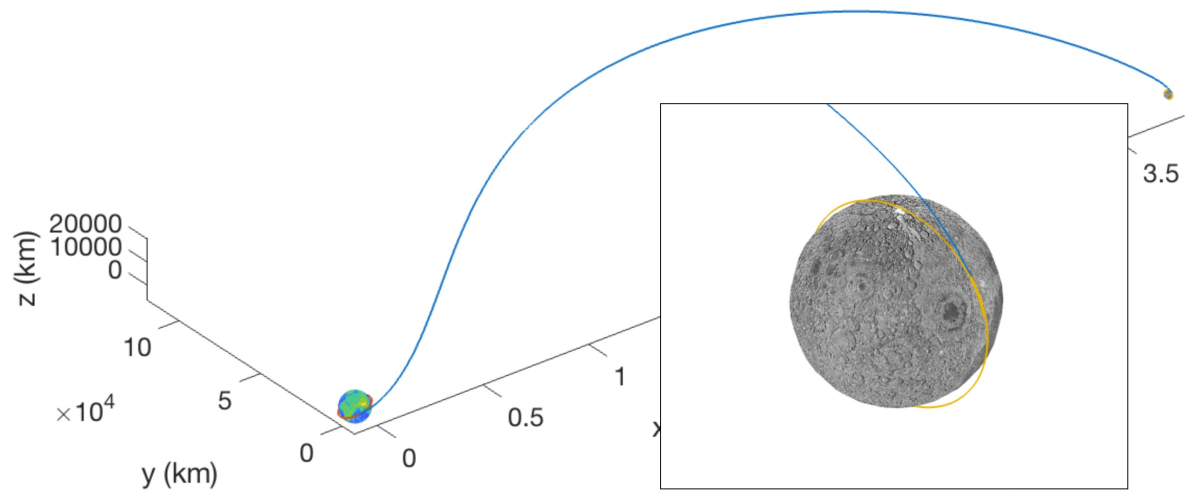

Figure 3: Plot of the 3D-trajectory in $\left(\hat{\imath},\hat{\jmath},\hat{k}\right)$ (with arrival at polar LMO in the inset)

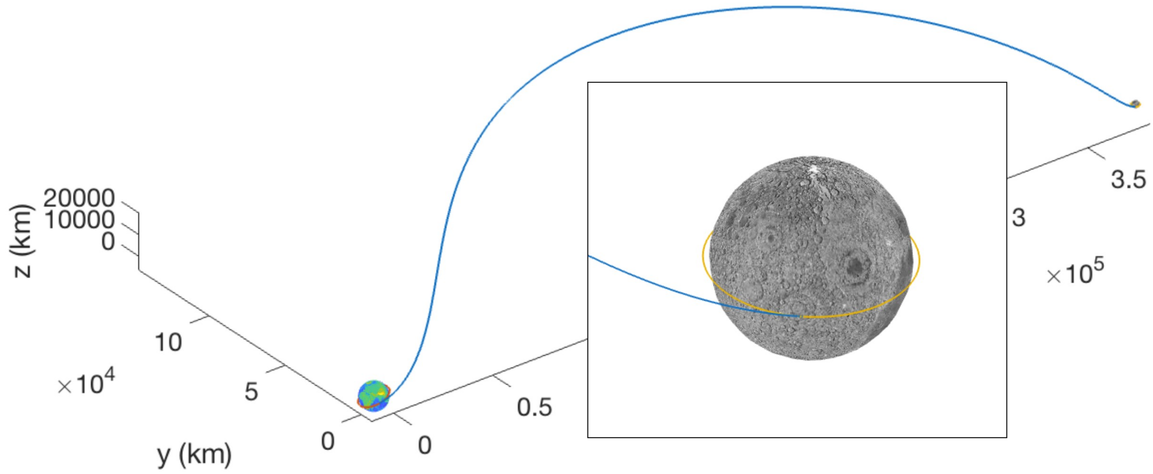

Figure 4: Plot of the 3D-trajectory in $\left(\hat{\imath},\hat{\jmath},\hat{k}\right)$ (with arrival at equatorial LMO in the inset)

i_{LMO} (deg)	J (km/s)	Δv_{LEO} (km/s)	Ω_{LEO} (deg)	α_i (deg)
90	3.89445	3.06812	-12.05	121.32
80	3.89376	3.06784	-11.44	122.42
70	3.89278	3.06750	-12.91	119.75
60	3.89162	3.06713	-11.15	122.48
50	3.89028	3.06677	-12.47	119.69
40	3.88906	3.06644	-12.60	118.78
30	3.88802	3.06616	-12.53	117.96
20	3.88731	3.06598	-11.32	118.89
10	3.88713	3.06593	-12.21	115.97
0	3.88796	3.06606	-11.59	115.16

Table 2: Results for the three-dimensional LEO-LMO orbit transfer

5 CONCLUDING REMARKS

This work addresses the problem of identifying minimum-fuel two- and three-dimensional orbit transfers from a specified low Earth orbit (LEO) to a low Moon orbit (LMO), under the assumption of employing high thrust-propulsion. The problem at hand is solved in the dynamical framework of the circular restricted problem of three bodies. First, the optimal two-dimensional orbit transfer from LEO to LMO is formulated in terms of two unknown parameters, and all the feasible transfers are identified. Then, the globally optimal two-impulse transfer is found, and is proven to be located at the boundary of the feasible region of the search space associated with Earth-Moon transfers. As a second step, three-dimensional transfers are considered, using a dynamical model that includes also the Cassini's laws of lunar motion. Several two-impulse optimal orbit transfers are identified, corresponding to distinct final lunar orbits. Selection of the initial optimal RAAN can benefit from precession of the orbit plane due to Earth oblateness. The propellant consumption associated with three-dimensional transfers turns out to be relatively insensitive to the final orbit inclination and exceeds only marginally the value of the globally optimal two-dimensional orbit transfer.

REFERENCES

[1] V. Szebehely. *Theory of Orbits in the Restricted Problem of Three Bodies*. Academic Press, London (1967).

[2] M. Pontani, P. Teofilatto. Polyhedral representation of invariant manifolds applied to orbit transfers in the Earth-Moon system. *Acta Astronautica*, Vol. 119, pp. 218-232 (2016).

[3] C. A. Kluever, B. L. Pierson. Optimal Earth-Moon trajectories using nuclear electric propulsion. *Journal of Guidance, Control, and Dynamics*, Vol. 20, No. 2, pp. 239-245 (1997).

[4] C. A. Kluever. Optimal Earth-Moon trajectories using combined chemical-electric propulsion. *Journal of Guidance, Control, and Dynamics*, Vol. 20, No. 2, pp. 253-258 (1997).

[5] M. Pontani, B. Conway. Particle Swarm Optimization Applied to Space Trajectories. *Journal of Guidance, Control, and Dynamics*, Vol. 33, No. 5, pp. 1429-1441 (2010).

[6] A. Miele, S. Mancuso. Optimal Trajectories for Earth-Moon-Earth Flight. *Acta Astronautica*, Vol. 49, No. 2, pp. 59-71 (2001).

[7] A. E. Roy. *Orbital Motion*. IOP Publishing Ltd., London (2005).